

Properties of K,Rb-intercalated C60 encapsulated inside carbon nanotubes called peapods derived from nuclear magnetic resonance

R. Mahfouz, M. Bouhrara, Y. Kim, T. Wågberg, C. Goze-Bac, and E. Abou-Hamad

Citation: *Journal of Applied Physics* **118**, 114305 (2015); doi: 10.1063/1.4931146

View online: <http://dx.doi.org/10.1063/1.4931146>

View Table of Contents: <http://scitation.aip.org/content/aip/journal/jap/118/11?ver=pdfcov>

Published by the *AIP Publishing*

Articles you may be interested in

[13C NMR on intercalated 2D-polymerised C60 and modified peapods](#)

AIP Conf. Proc. **723**, 238 (2004); 10.1063/1.1812081

[Charge transfer in intercalated C60 peapods](#)

AIP Conf. Proc. **633**, 118 (2002); 10.1063/1.1514087

[A multiple-quantum nuclear magnetic resonance study of interstitial Li clusters in Li x C 60](#)

J. Chem. Phys. **115**, 472 (2001); 10.1063/1.1377014

[Evidence for orientational tunneling of CO intercalated in C 60 : A nuclear magnetic resonance study](#)

J. Chem. Phys. **113**, 5141 (2000); 10.1063/1.1312866

[Dynamics of poly\(oxyethylene\) melts: Comparison of 13C nuclear magnetic resonance spin-lattice relaxation and dielectric relaxation as determined from simulations and experiments](#)

J. Chem. Phys. **106**, 3798 (1997); 10.1063/1.473433

The logo for AIP APL Photonics is displayed. It features the letters 'AIP' in a large, white, sans-serif font on the left, followed by a vertical line and the words 'APL Photonics' in a smaller, white, sans-serif font on the right. The background is a vibrant red with a bright yellow sunburst effect emanating from the top right corner.

APL Photonics is pleased to announce
Benjamin Eggleton as its Editor-in-Chief



Properties of K,Rb-intercalated C_{60} encapsulated inside carbon nanotubes called peapods derived from nuclear magnetic resonance

R. Mahfouz,¹ M. Bouhrara,² Y. Kim,³ T. Wågberg,⁴ C. Goze-Bac,⁵ and E. Abou-Hamad^{6,a)}

¹*Division of Physical Sciences & Engineering, King Abdullah University of Science and Technology, Thuwal, Saudi Arabia*

²*Department of Chemistry, School of Science and Technology, Nazarbayev University, 010000 Astana, Republic of Kazakhstan*

³*Department of Materials Science and Engineering, University of Pennsylvania, Philadelphia, Pennsylvania 19104, USA*

⁴*Department of Physics, Umeå University, 901 87 Umeå, Sweden*

⁵*nanoNMR Group, UMR5587, Université Montpellier II, Place E. Bataillon, 34095 Montpellier, Cedex 5, France*

⁶*KAUST Catalysis Center (KCC) King Abdullah University of Science and Technology, Thuwal, Saudi Arabia*

(Received 9 June 2015; accepted 5 September 2015; published online 18 September 2015)

We present a detailed experimental study on how magnetic and electronic properties of Rb,K-intercalated C_{60} encapsulated inside carbon nanotubes called peapods can be derived from ^{13}C nuclear magnetic resonance investigations. Ring currents do play a basic role in those systems; in particular, the inner cavities of nanotubes offer an ideal environment to investigate the magnetism at the nanoscale. We report the largest diamagnetic shifts down to -68.3 ppm ever observed in carbon allotropes, which is connected to the enhancement of the aromaticity of the nanotube envelope upon intercalation. The metallization of intercalated peapods is evidenced from the chemical shift anisotropy and spin-lattice relaxation (T_1) measurements. The observed relaxation curves signal a three-component model with two slow and one fast relaxing components. We assigned the fast component to the unpaired electrons charged C_{60} that show a phase transition near 100 K. The two slow components can be rationalized by the two types of charged C_{60} at two different positions with a linear regime following Korringa behavior, which is typical for metallic system and allow us to estimate the density of state at Fermi level $n(E_F)$. © 2015 AIP Publishing LLC.

[<http://dx.doi.org/10.1063/1.4931146>]

I. INTRODUCTION

Carbon nanotubes have attracted attention due to their extraordinary structural, mechanical, magnetic, and electronic properties, which make them interesting for various applications in our daily life.¹⁻³

Ever since the discovery of C_{60} encapsulated inside single-walled carbon nanotubes (SWNTs) called peapods,⁴ SWNTs have been proposed as potential ultra clean nano reactors^{5,6} or gas transport systems.⁷ They can be filled not only by C_{60} but also with many other molecules like, e.g., pentacene,⁸ metallocenes,⁹ hexamethylelamine,¹⁰ and C_{70} .¹¹ However, only very few attempts have been made to modify encapsulated species. At present, these are intercalation of C_{60} with alkali metals,¹² high pressure polymerization of C_{60} ,^{13,14} insertion of C_{60} inside double-walled carbon nanotubes (DWNTs),¹⁵ and catalyst growth of nanotubes inside SWNTs.¹⁶ Tuning the electronic and magnetic properties of peapods is of paramount scientific and technological interest. One of the ways to proceed is to intercalate peapods with alkali metals, which is known to change the electronic and magnetic properties of the peapods due to electron transfer from the alkali atoms to the peapods. Despite the progress

made in the last decade, there are still many open questions concerning this transfer.

Nuclear magnetic resonance (NMR) has shown to be an excellent tool for characterizing fullerenes, fullerenes inside carbon nanotubes, graphite, and conducting polymers.¹⁷⁻³⁰ For carbon nanotubes studies, ^{13}C NMR has not been used as frequently, although some studies have been reported recently to study their structural properties,²⁵ their electronic properties,^{26,27,29} their magnetic properties,²² or the dynamic properties of molecules encapsulated inside carbon nanotubes.^{20,21}

In this work, we provide additional data in detail on how the intercalation of peapods with alkali metals influences the magnetic and electronic properties. The ^{13}C MAS NMR spectrum revealed the diamagnetic shielding from outer tubes that can be interpreted in terms of the magnetism of the carbon honeycomb structure with the retention and the destruction of delocalized π ring currents circulating around the outer nanotube. This phenomenon is universal and even enhanced in the case of the sample corresponding to K, Rb-intercalated peapods for which the outer SWNTs are charged with electrons transferred from the alkali. The shift anisotropy (CSA) NMR spectra and spin-lattice relaxation studies revealed the metallic properties and allowed us to estimate the values of the density of state (DOS) at Fermi level $n(E_F)$.

^{a)}Author to whom correspondence should be addressed. Electronic mail: edy.abouhamad@kaust.edu.sa

II. EXPERIMENTAL PROCEDURES

The starting materials, SWNTs and 25% ^{13}C enriched C_{60} , were purchased from Carbon Solution, Inc., and MER Corporation, respectively. The magnetic purification is well described in Ref. 31. Briefly, SWNTs were oxidized in air for 10 min at 600°C , followed by a bath sonication in hydrochloric acid for 40 min at 650°C to remove bare Ni/Y catalyst particles. After the acid treatment, materials were dispersed in dimethylformamide (DMF) by bath sonication; the solution was filtered through the magnetic field of 1.1 T. Afterwards, peapods was prepared by vapor phase filling for 10 h at 650°C , followed by 1 h post annealing in dynamic vacuum to remove excessive enriched fullerenes. The Rb and K-intercalated peapods can be found in Refs. 32 and 33. The intercalation proceeds by saturating peapods by Rb or K vapor transport onto degassed peapods at 200°C in a cycled process for 10 days. Once the doping was achieved, the excess of doping was removed, and the sample was rinsed by internal distillation and then dried by cooling the ampoule at -70°C .

The ^{13}C NMR experiments were carried out in Montpellier using a Bruker ASX200 spectrometer at magnetic field of 4.2 T and Larmor frequency of 50.3 MHz. The ^{13}C NMR spectrum was performed using Han echo synchronized with a rotor spinning at 10 kHz. The spin-lattice relaxation time was measured by saturation-recovery technique. Temperature studies in NMR were performed in a sealed glass tube after being evacuated overnight at a dynamic vacuum of 10^{-8} Torr.

III. RESULTS AND DISCUSSION

Figure 1(a) shows the high resolution MAS ^{13}C NMR spectra of magnetically purified SWNTs encapsulated with C_{60} called peapods compared to the K and Rb intercalated peapods. According to the natural abundance of 1.1% of ^{13}C in the outer nanotube, the 25% of ^{13}C in the enriched encapsulated C_{60} , and a filling factor of 70% of the inner cylindrical space of the SWNTs, the contribution to the total NMR signal intensity from the outer nanotube in the spectra is estimated to be 16%. Consequently, these NMR spectra are dominated by the signal from the encapsulated molecules. For non-intercalated peapods in Figures 1(a-I), the signal can be fitted with three lines: the first at 111.3 ppm (β -position), a second at 118.8 ppm, and a third at 148.2 ppm (α -position).

The β line at 111.3 ppm is assigned to C_{60} molecules in the interior of the SWNT. This signal is diamagnetically shifted from the normal position of fcc- C_{60} located at 143.6 ppm. The diamagnetic shift occurs due to a local magnetic field on the C_{60} molecules produced by ring currents on the honeycomb surface of the nanotube.^{20,21} The sharp character of this line indicates that the C_{60} molecules are still rotating inside the carbon nanotubes.²¹ The signal at 118.8 ppm represents the NMR response of the carbons in the SWNTs.²³ Finally, the α line at 148.2 ppm represents C_{60} molecules at the interior of SWNT but located at tube defects, giving rise to a slight paramagnetic shift of the NMR line position compared to pristine C_{60} . Its significant broadening compared to freely rotating C_{60} suggests that the C_{60} molecules are no longer rotating when located in the vicinity of nanotube defects. The broadening indicates also that C_{60} molecules are not located outside the SWNT, which would show up as a narrow line at 143.6 ppm.

The K, Rb-intercalated peapods was tested by exposing the samples to air, and a series of MAS ^{13}C NMR spectra had been taken without any change after several days. The K and Rb-intercalated peapods in Figure 1(a)-II and III, respectively, results in drastic modification of the NMR spectra compared to the non-intercalated peapods. The signals of the different contributions keep their ratio as in peapods, but the line position and FWHM have changed. A tutorial fit with three lines, the first at 117 ppm (β -position), a second at 128 ppm, and a third at 185.3 ppm (α -position), of the ^{13}C NMR spectrum of the Rb-intercalated peapod sample is given in Figure 1(b). The line at 128 ppm represents the outer SWNTs, which exhibit a clear paramagnetic shift of about 10 ppm when comparing to the pristine SWNTs, indicating a transition into a metallic state. A comparable paramagnetic shift was also observed on lithium³⁰ and Cs-intercalated SWNTs.^{26,27,29} The line α of C_{60} close to defects on outer nanotubes at the position δ_α (185.3 ppm) shows a clear second paramagnetic shift compared to the non-intercalated peapods. The ^{13}C NMR shifts are similar to that in AC_{60} , A_2C_{60} , A_3C_{60} , and A_4C_{60} compounds due to the intercalation of the C_{60} molecules.³³⁻⁴⁰ The second line β at the position δ_β (117 ppm) presents a larger diamagnetic shift in the range of $\Delta = \delta_\beta - \delta_\alpha = -68.3$ ppm compared to -36 ppm for non-intercalated peapods. Our results can be interpreted in terms of the magnetism of the carbon honeycomb structure with

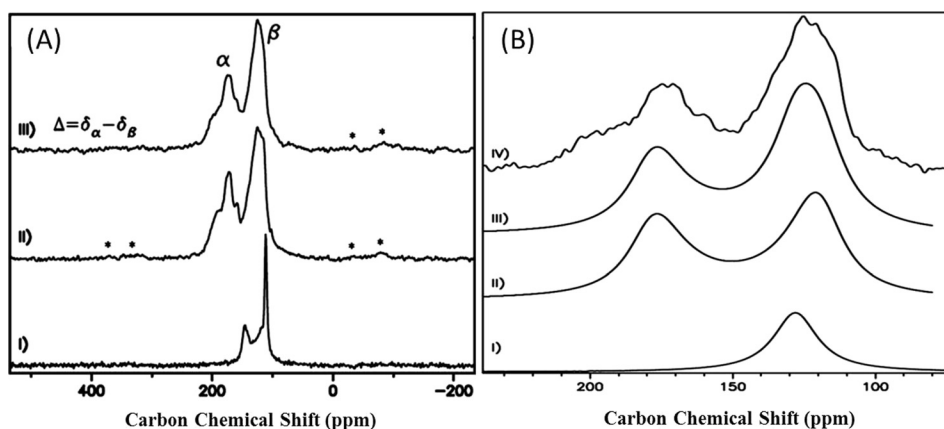


FIG. 1. (a) High resolution ^{13}C MAS NMR spectra spin at 10 kHz at room temperature (I) peapods, (II) K-intercalated peapods, (III) Rb-intercalated peapods. Stars indicate the side bands of the two isotropic shifts. (b) Fitting of Rb-intercalated peapods, (I) SWNT content, (II) paramagnetically and diamagnetically shifted fullerenes, (III) fitted curve, and (V) experimental NMR spectrum.

the retention and the destruction of delocalized π ring currents circulating around the outer nanotube. This phenomenon is universal and even enhanced in the case of the sample corresponding to K, Rb-intercalated peapods; it is caused by an extra electronic charge transferred from the alkali to create a bigger ring current.

The lines show substantial broadening, which can be a distribution of the shifts pointing to a very inhomogeneous wave function at $C_{60}^{(n-)}$ molecules. This is to be expected if the symmetry of the molecules is perturbed by intermolecular bonding. The characteristic feature of the spectrum proposes the polymerization or dimerization of $C_{60}^{(-n)}$ molecules,^{33,41} which can be confirmed by measuring vibrational properties using Raman spectroscopy. The presence of the rotational side bands suggests that the C_{60} molecules at α and β positions are no more rotating and they are static.

For more investigation about the electronic properties of the K, Rb-intercalated peapods, chemical shift anisotropy (CSA) and spin-lattice relaxation (T_1) with different temperatures were carried out. The static ^{13}C NMR spectra from the non-intercalated peapods (Figure 2(a)–I) as discussed before²⁰ have three main contributions: the typical powder line shape from SWNTs, the CSA tensor of static paramagnetically shifted C_{60} , and the rotating diamagnetically shifted C_{60} . The static ^{13}C NMR spectra from the K,Rb-intercalated peapods (Figure 2(a)) II and III, respectively, exhibit a clear change in the CSA compared to non-intercalated peapods and show a typical powder spectrum for a metallic system after intercalation. For the Rb-intercalated peapods (Fig. 2(b)), the line shape of the SWNTs shows a clear anisotropy reduction compared to pristine SWNTs due to change into metallic-like shift anisotropy as reported by Goze-Bac *et al.*²³ and Latil *et al.*²⁴ (Fig. 2(b)), I). The chemical shift anisotropy tensor of the static paramagnetically shifted C_{60} corresponds to a charged C_{60} molecules (Figure 2(b), II) and the blocked diamagnetically C_{60} corresponds also to a charge C_{60} (Figure 2(b), III).

In order to interpret our data, we developed the following analysis: The observed shift can be separated into two parts: the chemical shift σ and the Knight shift K , where σ and K are second rank tensors consisting of an isotropic and

an anisotropic part. The chemical shift σ arises from local orbital fields caused by local currents in the sample. The Knight shift K arises from the hyperfine coupling of conduction electron spins to unclear spins.⁴² The isotropic part of the Knight shift is paramagnetic and proportional to the probability density of the conduction electrons at the nucleus $|\Psi(0)|^2$ and the density of states at the Fermi level $n(E_F)$

$$K_{\text{iso}} = \frac{8\pi}{3} |\Psi(0)|^2 \mu_B^2 n(E_F). \quad (1)$$

However, it is not trivial to estimate $n(E_F)$ directly from the isotropic line position because of the unknown isotropic chemical shift in charged C_{60} . The ^{13}C shift distribution therefore arises from a broad distribution of knight shifts.

Both Knight shift K and T_1 relaxation are affected by the DOS at the Fermi surface $n(E_F)$, if shift and relaxation are dominated by the magnetic interaction with the conduction electrons of the metal.⁴²

At room temperature, the observed spin lattice relaxation curve signals (Figure 3(a)) a three component model time measurements on K and Rb-intercalated peapods. Indeed, the shape of MAS NMR spectrum of Rb-intercalated peapods (Figure 4) with different delays shows the obvious difference between the saturation of the C_{60} molecules at both α and β positions. We clearly observed that the C_{60} molecules at α position are saturated about 600 ms and the C_{60} molecules at β position are saturated about 3 s. The magnetization recovery, $M(t)$, with triple exponential function of the type

$$M = M_\alpha (1 - e^{-\frac{t}{T_{1\alpha}}}) + M_\beta (1 - e^{-\frac{t}{T_{1\beta}}}) + M_\gamma (1 - e^{-\frac{t}{T_{1\gamma}}}), \quad (2)$$

where M_α , M_β , and M_γ are the equilibrium magnetizations for the three components. The relative magnitudes, M_α/M_0 , M_β/M_0 , and M_γ/M_0 , with $M_0 = M_\alpha + M_\beta + M_\gamma$ do not differ in a systematic way and are determined to be $20\% \pm 5\%$, $36\% \pm 5\%$, and $44\% \pm 5\%$, respectively. The fit at room temperature results in $T_{1\alpha} = 60$ ms, $T_{1\beta} = 500$ ms, and $T_{1\gamma} = 2$ s for Rb-intercalated peapods (Figure 3(b)) and $T_{1\alpha} = 60$ ms, $T_{1\beta} = 700$ ms, and $T_{1\gamma} = 1.5$ s for K-intercalated peapods

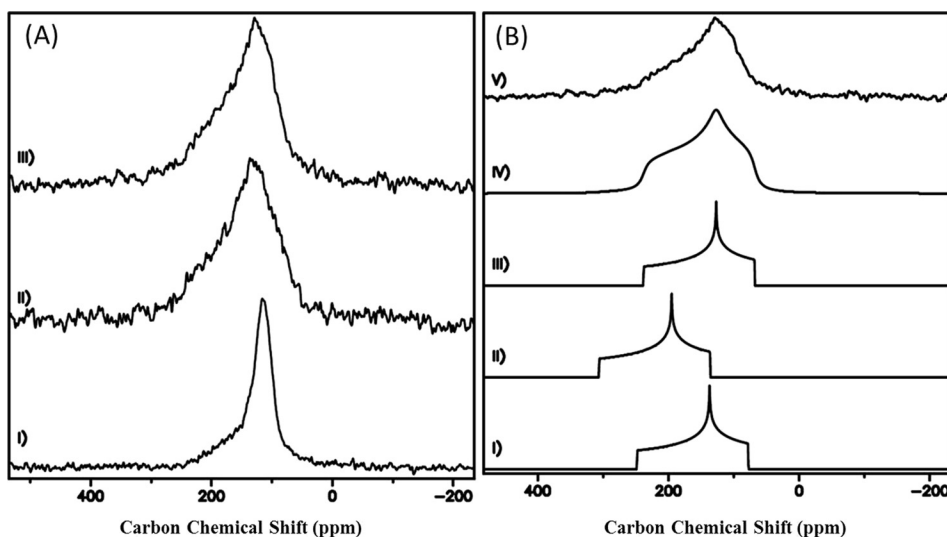


FIG. 2. (a) ^{13}C Static NMR spectrum at room temperature of (I) peapods, (II) K-intercalated peapods, and (III) Rb-intercalated peapods. (b) Fitting of the ^{13}C static NMR spectrum of Rb-intercalated peapods at room temperature (I) simulated CSA of SWNTs, (II) simulated CSA of C_{60} at α position, (III) simulated CSA of C_{60} at β position, (IV) sum of all fitting, and (V) the experimental static NMR spectrum.

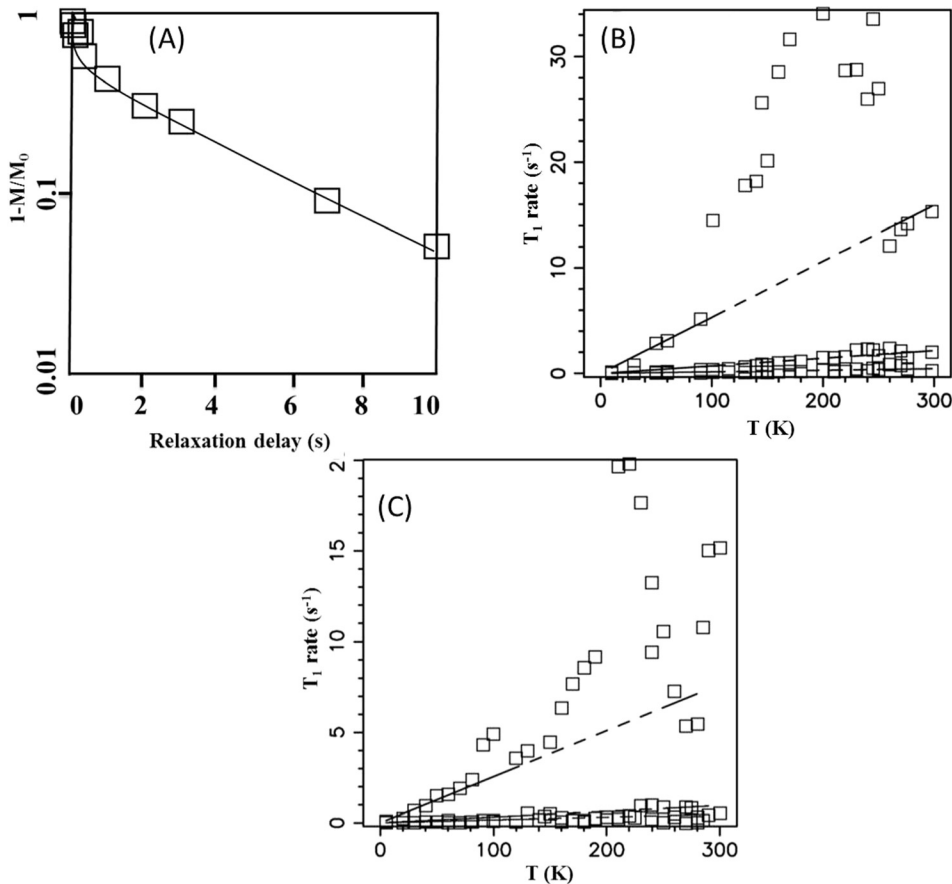


FIG. 3. (a) Magnetization recovery at room temperature of Rb-intercalated peapods and relaxation rate $1/T_1$ as a function of temperature of (B) Rb and (C) K-intercalated peapods.

(Figure 3(c)). We assigned the fast component to the unpaired electrons charged C_{60} in both α and β positions, and the spin-lattice relaxation value of 60 ms coincides with value found in the high temperature phase of AC_{60} .^{43,44} The two slow components at 500 ms and 2 s are assigned to the charged C_{60} on α and β positions, respectively, consist with the MAS NMR spectrum with different delays (Figure 4). Spin lattice relaxation time about a few seconds is comparable to the value obtained for AC_{60} at low temperature in the polymeric phase.^{43,44} The values obtained suggest that large spin-density distributions on C_{60} molecules propose the polymerization of the charged C_{60} . Figures 3(b) and 3(c) show

the T_1 measurements as a function of temperature for Rb and K-intercalated peapods, respectively. The relaxation rate for the fast component shows a phase transition near 100 K with change in their electronic properties. At temperature above 100 K, the T_1 is so fast, which can be explained by the paramagnetic properties of C_{60} at this phase with exchange coupling between electrons spins that are localized on C_{60} ions. The unpaired electrons are principally localized on individual C_{60} molecules with exchange coupling between localized electron spins and the electrons fluctuate rapidly that dominate the electronics dynamics. Also, there is a small electron probability density which produces a Fermi contact hyperfine

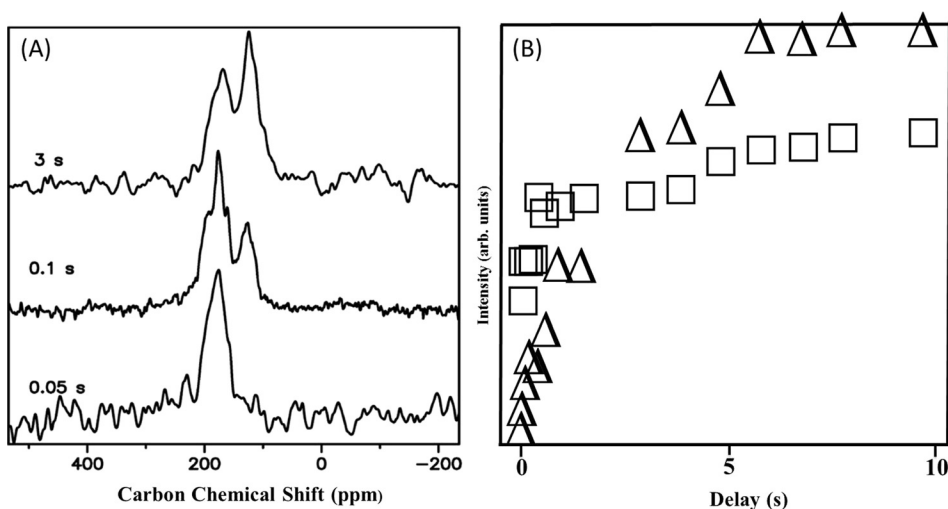


FIG. 4. (a) ^{13}C MAS NMR spectrum of Rb-intercalated peapods at different delays and (b) the intensity of both isotropic shifts with delays.

coupling which is non zero due to the polarization of the electron spins in the applied magnetic field produce a temperature dependent inhomogeneous. The long time scale of the phase separation caused by Rb^+ and K^+ diffusion affects the relaxation, announcing that the alkali is fully ionized as seen in Figure 5, which gives a chemical shift at 0 ppm in the ^{87}Rb MAS NMR, and the position of the line around 0 ppm observed by ^{133}Cs NMR of Cs-intercalated SWNTs at low intercalation levels suggests the existence of one Cs site in the SWNTs.²⁹ Probably, the intercalation site is the interstitial channel between three tubes in a bundle, which exhibits a very weak hyperfine coupling and are fully ionized; and therefore, a simple charge transfer is applicable.²⁷ More ^{87}Rb NMR MAS, spin-lattice (T_1), and spin-spin (T_2) with different temperatures and Raman studies will be done in the future to check the intercalation positions of the alkali metals. At temperature below 100 K, the relaxation rate is substantially smaller, which showed that the electrons spin susceptibility is reduced in this phase and the most unpaired electron spins that are apparently become paired probably provide polymerization of C_{60} ions. For the two slow components that are assigned to the C_{60} molecules at α and β positions, we observe a linear regime following Korringa behavior, which is typical for metallic system.^{33,45} The ^{13}C NMR T_1 measurements as a function of temperature in Figures 3(b) and 3(c) can be expressed as

$$\frac{1}{T_1} = \frac{2\pi k_B}{\hbar} A_{\text{iso}}^2 n(E_F)^2, \quad (3)$$

where A_{iso} is the isotropic hyperfine coupling constant.⁴⁶ We assume a hyperfine coupling of $A_{\text{iso}} = 8.2 \times 10^{-7}$ eV and fit the linear regime part of the ^{13}C NMR spin lattice relaxation. Hence, we were able to estimate the $n(E_F)$ for the two components as reported in Table I.

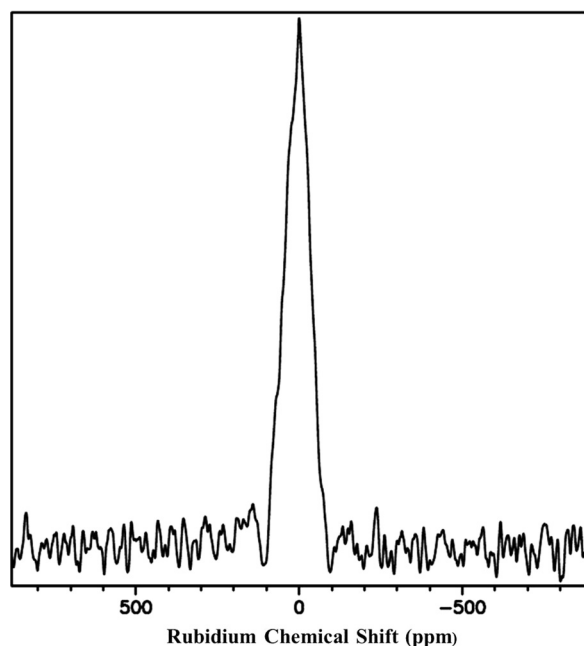


FIG. 5. ^{87}Rb NMR spectra of Rb-intercalated peapods.

TABLE I. Density of states at the Fermi level $n(E_F)$ for Rb and K-intercalated peapods.

	Rb-intercalated peapods	K-intercalated peapods
$n(E_F)$ for fast relaxation below 100 K	0.3	0.2
$N(E_F)$ for slow relaxation at α position	0.1	0.09
$n(E_F)$ for slow relaxation at β position	0.05	0.05

IV. CONCLUSION

Using 25% ^{13}C enriched C_{60} by which the effect of dipolar coupling could be minimized enables us to investigate the local magnetic and electronic properties of Rb,K-intercalated peapods. ^{13}C NMR intercalated peapods produced three well resolved isotropic shifts: the line α of C_{60} close to defects on outer nanotubes that shows a clear paramagnetic shift, the second line β C_{60} in the interior of the tubes at the position δ_β (117 ppm) presents a larger diamagnetic shift in the range of $\Delta = \delta_\beta - \delta_\alpha = -68.3$ ppm that can be interpreted in terms of the magnetism of the carbon honeycomb structure with the retention and the destruction of delocalized π ring currents circulating around the outer nanotube, and the line at 128 ppm representing the outer SWNTs that exhibit a clear paramagnetic shift, indicating a transition into a metallic state. The shift anisotropy (CSA) change into metallic-like shift corresponds to charged C_{60} molecules.

The spin-lattice relaxation studies on intercalated peapods reveal a three component model with one very fast relaxing assigned to the unpaired electrons charged C_{60} and two slow relaxing components that can be assigned to the C_{60} molecules at α and β positions. The relaxation rate for the fast component shows a phase transition near 100 K, and for the two slow components, we observe a linear regime following Korringa behavior, which is typical for metallic system and allow us to estimate the density of state at Fermi level $n(E_F)$.

¹J. W. Mintmire, B. I. Dunlap, and C T. White, *Phys. Rev. Lett.* **68**, 631 (1992).

²R. Saito, M. Fujita, G. Dresselhaus, and M. S. Dresselhaus, *Appl. Phys. Lett.* **60**, 2204 (1992).

³J. G. Wildoer, L. C. Venema, A. G. Rinzler, R. E. Malley, and C. Dekker, *Nature* **391**, 59 (1998).

⁴B. W. Smith, M. Monthieux, and D. E. Luzzi, *Nature (London)* **396**, 323–324 (1998).

⁵E. Dujardin, T. W. Ebbesen, H. Hiura, and K. Tanigaki, *Science* **265**, 1850–1852 (1994).

⁶R. Pfeiffer, H. Kuzmany, Ch. Kramberger, Ch. Schaman, T. Pichler, H. Kataura, Y. Achiba, J. Kürti, V. Zólyomi *et al.*, *Phys. Rev. Lett.* **90**, 225501 (2003).

⁷A. I. Skoulidas, D. M. Ackerman, J. K. Johnson, and D. S. Sholl, *Phys. Rev. Lett.* **89**, 185901 (2002).

⁸T. Takenobu, T. Takano, M. Shiraishi, Y. Murakami, M. Ata, H. Kataura, Y. Achiba, and Y. Iwasa, *Nature Mater.* **2**, 683–688 (2003).

⁹L. J. Li, A. N. Khlobystov, J. G. Wiltshire, G. A. D. Briggs, and R. J. Nicholas, *Nature Mater.* **4**, 481–485 (2005).

¹⁰Y. Ren and G. Pastorin, *Adv. Mater.* **20**, 2031–2036 (2008).

¹¹A. N. Khlobystov, R. Scipioni, D. Nguyen-Manh, D. A. Britz, D. G. Pettifor, G. Andrew, and D. Briggs, *Appl. Phys. Lett.* **84**(5) 792 (2004).

- ¹²T. Pichler, A. Kukovec, H. Kuzmany, H. Kataura, and Y. Achiba, *Phys. Rev. B* **67**, 125416 (2003).
- ¹³S. Kawasaki, T. Hara, T. Yokomae, F. Okino, H. Touhara, H. Kataura, T. Watanuki, and Y. Ohishi, *Chem. Phys. Lett.* **418**, 260–263 (2006).
- ¹⁴Y. Zou, B. Liu, M. Yao, Y. Hou, L. Wang, S. Yu, P. Wang, B. Li, B. Zou, T. Cui, G. Zou, T. Wågberg, and B. Sundqvist, *Phys. Rev. B* **76**, 195417 (2007).
- ¹⁵Y. J. Dappe and R. Scipioni, *Phys. Rev. B* **84**, 193409 (2011).
- ¹⁶H. Shiozawa, T. Pichler, A. Gruneis, R. Pfeiffer, H. Kuzmany, Z. Liu, K. Suenaga, and H. Kataura, *Adv. Mater.* **20**, 1443–1449 (2008).
- ¹⁷A. Pasquarello, M. Schlüter, and R. C. Haddon, *Science* **257**, 1660 (1992).
- ¹⁸R. C. Haddon, *Nature (London)* **378**, 249 (1995).
- ¹⁹G.-W. Wang, B. R. Weedon, M. S. Meier, M. Saunders, and R. J. Cross, *Org. Lett.* **2**, 2241 (2000).
- ²⁰E. Abou-Hamad, Y. Kim, A. V. Talyzin, C. Goze-Bac, D. Luzzi, A. Rubio, and T. Wågberg, *J. Phys. Chem. C* **113**, 8583 (2009).
- ²¹E. Abou-Hamad, Y. Kim, T. Wågberg, D. Boesch, S. Aloni, A. Zettl, A. Rubio, and C. Goze-Bac, *ACS Nano* **3**(12), 3878 (2009).
- ²²Y. Kim, E. Abou-Hamad, A. Rubio, T. Wågberg, A. V. Talyzin, D. Boesch, S. Aloni, A. Zettl, D. E. Luzzi, and C. Goze-Bac, *J. Chem. Phys.* **132**, 021102 (2010).
- ²³C. Goze-Bac, S. Latil, P. Lauginie, V. Jourdain, J. Conard, L. Duclaux, A. Rubio, and P. Bernier, *Carbon* **40**, 1825 (2002).
- ²⁴S. Latil, L. Henrard, C. Goze-Bac, P. Bernier, and A. Rubio, *Phys. Rev. Lett.* **86**, 3160 (2001).
- ²⁵E. Abou-Hamad, M.-R. Babaa, M. Bouhrara, Y. Kim, Y. Saih, S. Dennler, F. Mauri, J.-M. Basset, C. Goze-Bac, and T. Wågberg, *Phys. Rev. B* **84**, 165417 (2011).
- ²⁶E. Abou-Hamad, C. Goze-Bac, F. Nitze, M. Schmid, R. Aznar, M. Mehring, and T. Wågberg, *New J. Phys.* **13**, 053045 (2011).
- ²⁷M. Bouhrara, Y. Saih, T. Wågberg, C. Goze-Bac, and E. Abou-Hamad, *J. Appl. Phys.* **110**, 054306 (2011).
- ²⁸M. Bouhrara, E. Abou-Hamad, G. Alabedi, I. Al-Taie, Y. Kim, T. Wågberg, and C. Goze-Bac, *J. Nanomater.* **2013**, 713475 (2013).
- ²⁹M. Schmid, R. Mahfouz, M. Bouhrara, Y. Saih, M. Mehring, J.-M. Basset, C. Goze-Bac, and E. Abou-Hamad, *Carbon* **50**, 5292–5300 (2012).
- ³⁰M. Schmid, C. Goze-Bac, S. Kramer, S. Roth, M. Mehring, C. Mathis, and P. Petit, *Phys. Rev. B* **74**, 073416 (2006).
- ³¹Y. Kim, O. N. Torrens, J. M. Kikkawa, E. Abou-Hamad, C. Goze-Bac, and D. Luzzi, *Chem. Mater.* **19**(12), 2982 (2007).
- ³²R. R. Meyer, J. Sloan, R. E. Dunin-Borkowski, A. I. Kirkland, M. C. Novotny, S. R. Bailey, J. L. Hutchison, and M. L. H. Green, *Science* **289**, 1324 (2000).
- ³³T. Pichler, H. Kuzmany, H. Kataura, and Y. Achiba, *Phys. Rev. Lett.* **87**, 267401 (2001).
- ³⁴R. E. Walstedt, D. W. Murphy, and M. Rosseinsky, *Nature* **362**, 611–613 (1993).
- ³⁵F. Rachdi, L. Hajji, M. Galtier, T. Yildirim, J. E. Fischer, C. Goze, and M. Mehring, *Phys. Rev. B* **56**, 7831 (1997).
- ³⁶C. Goze, F. Rachdi, and M. Mehring, *Phys. Rev. B* **54**, 5164 (1996).
- ³⁷J. Reichenbach, F. Rachdi, I. Luk'yanchuk, M. Ribet, G. Zimmer, and M. Mehring, *J. Chem. Phys.* **101**, 4585 (1994).
- ³⁸K.-F. Thier, C. Goze, M. Mehring, F. Rachdi, T. Yildirim, and J. E. Fischer, *Phys. Rev. B* **59**, 10536 (1999).
- ³⁹T. Yildirim, L. Barbedette, J. E. Fischer, G. M. Bendele, P. W. Stephens, C. L. Lin, C. Goze, F. Rachdi, J. Robert, P. Petit, and T. T. M. Palstra, *Phys. Rev. B* **54**, 11981 (1996).
- ⁴⁰G. Zimmer, M. Mehring, C. Goze, and F. Rachdi, *Phys. Rev. B* **52**, 13300 (1995).
- ⁴¹C. Goze, F. Rachdi, L. Hajji, M. Núñez-Regueiro, L. Marques, J.-L. Hodeau, and M. Mehring, *Phys. Rev. B* **54**, R3676(R) (1996).
- ⁴²O. V. Yazye and L. Helm, *Phys. Rev. B* **72**, 245416 (2005).
- ⁴³D. Bormann, J. L. Sauvajol, C. Goze, F. Rachdi, A. Moreac, A. Girard, L. Forro, and O. Chauvet, *Phys. Rev. B* **54**, 14139 (1996).
- ⁴⁴H. Alloul, V. Brouet, E. Lafontaine, L. Malier, and L. Forro, *Phys. Rev. Lett.* **76**, 2922 (1996).
- ⁴⁵R. Tyck, G. Dabbagh, M. J. Rosseinsky, D. W. Murphy, R. M. Fleming, A. P. Ramirez, and J. C. Tully, *Science* **253**(5022), 884–886 (1991).
- ⁴⁶X. P. Tang, A. Kleinhammes, H. Shimoda, L. Fleming, K. Y. Bennoune, S. Sinha, C. Bower, O. Zhou, and Y. Wu, *Science* **288**, 492 (2000).